ARTICLE

Tuning the Packing Density of 2D Supramolecular Self-Assemblies at the Solid–Liquid Interface Using Variable Temperature

Camille Marie,[†,‡] Fabien Silly,[†,‡] Ludovic Tortech,[†,‡] Klaus Müllen,[§,*] and Denis Fichou[†,‡,*]

[†]CEA, Nanostructures et Semi-Conducteurs Organiques, SPCSI, F-91191 Gif-sur-Yvette, France, [‡]IPCM, UMR CNRS 7201, Université Pierre et Marie Curie, 4 place Jussieu, 75005 Paris, France, and [§]Max-Planck Institute for Polymer Research, Ackermanweg 10, 55128 Mainz, Germany

ABSTRACT The two-dimensional (2D) crystal engineering of molecular architectures on surfaces requires controlling various parameters related respectively to the substrate, the chemical structure of the molecules, and the environmental conditions. We investigate here the influence of temperature on the self-assembly of hexakis(*n*-dodecyl)-*peri*-hexabenzocoronene (HBC-C_{12}) adsorbed on gold using scanning tunneling microscopy (STM) at the liquid/solid interface. We show that the packing density of 2D self-assembled HBC-C_{12} can be precisely tuned by adjusting the substrate temperature. Increasing the temperature progressively over the 20–50 °C range induces three irreversible phase transitions and a 3-fold increase of the packing density from 0.111 to 0.356 molecule/nm^2. High-resolution STM images reveal that this 2D packing density increase arises from the stepwise desorption of the *n*-dodecyl chains from the gold surface. Such temperature-controlled irreversible phase transitions are thus a versatile tool that can then be used to adjust the packing density of highly ordered functional materials in view of applications in organic electronic devices.

KEYWORDS: scanning tunneling microscopy · self-assembly · supramolecular · temperature · phase diagram

Intense research effort is focusing on the control of the arrangement of organic molecules on surfaces in view of developing novel nanostructured functional materials.[1–8] The two-dimensional (2D) self-assembly of appropriate molecular building blocks, that is the control of directional interactions between predesigned molecules and the substrate, is a successful strategy which has recently led to a variety of periodic patterns.[9,10] The 2D crystal engineering of molecular architectures on atomically flat surfaces requires the control of three types of parameters related, respectively, to the substrate, the chemical structure of the molecules, and the environmental conditions. Substrate parameters such as surface reconstruction,[11–14] electronic properties,[15] and surface modification by overlayers[6,16,17] strongly influence the structural arrangement of the self-assembly. In comparison, molecular parameters permit the orientation of 2D molecular packing by exploiting noncovalent intermolecular interactions such as van der Waals interactions,[18,19] hydrogen bonds,[20–26] and π-stacking.[27,28] Finally, external and environmental parameters such as light irradiation,[29] electric and magnetic fields,[30,31] time,[32,33] concentration,[34,35] ratio,[36] and temperature[37–41] also proved to be key players governing supramolecular self-assemblies.

A number of studies have been reported on the influence of time and temperature on 2D molecular networks. However, most of them have been performed in ultrahigh vacuum[38–40] and very few at the liquid/solid interface.[32,33,37,41] For example, we recently reported on the time evolution of the 2D packing of hexakis(*n*-dodecyl)-*peri*-hexabenzocoronene (HBC-C_{12}) adlayers in heteroepitaxy on *n*-pentacontane monolayers at the *n*-tetradecane/graphite interface.[32] In contrast to time, temperature is a versatile physical parameter which can be precisely adjusted so that a particular 2D arrangement is formed and retained. In particular, temperature is essential to tune the 2D packing density and obtain a material with desired electronic properties.

We show here by scanning tunneling microscopy (STM) that the packing density of HBC-C_{12} self-assembled at the Au(111)-$(22\times\sqrt{3})$/*n*-tetradecane interface can be tuned by varying the substrate temperature. Increasing the temperature from 20 to 50 °C induces three successive and irreversible structural transitions accompanied by a 3-fold increase of the HBC-C_{12} packing density. High-resolution STM images reveal that this 2D packing density increase arises

*Address correspondence to denis.fichou@cea.fr, muellen@mpip-mainz.mpg.de.

Received for review November 27, 2009 and accepted February 10, 2010.

Published online February 15, 2010. 10.1021/nn901717k

from the stepwise desorption of the *n*-dodecyl chains from the gold surface.

RESULTS AND DISCUSSION

At room temperature (20 °C) HBC-C_{12} molecules initially form an open network, the α-phase, having a rhombic unit cell with lattice parameters $a = b =$ 3.6 nm and $\theta \approx 70°$ (Figure 1). Two *n*-tetradecane molecules are coadsorbed in-between neighboring HBC-C_{12} molecules (see Figure 1b,c), the HBC-C_{12}/*n*-tetradecane ratio being 1:4 and the HBC-C_{12} packing density being 0.082 molecule/nm^2. Note that in the α-phase two *n*-dodecyl chains are not lying on the surface (gray spots in Figure 1c). Finally, the α-phase coexists with an *n*-tetradecane monolayer as it can be observed in the upper right corner of Figure 1a.

The initial α structure rapidly evolves into another arrangement, the β-phase (Figure 2). The complete disappearance of the α-phase occurs 1 h after deposition and the β-phase is the only arrangement observed on the surface. This shows that the α-phase is not stable at room temperature. The close-packed β-network has a rhombic unit cell with lattice parameters $a = b =$ 3.0 nm and $\theta \approx 87°$, the HBC-C_{12}/*n*-tetradecane ratio being 1:2 and the packing density being 0.111 molecule/nm^2.

By heating at 30 °C a third phase appears (Figure 3). The corresponding γ-network has a parallelogram unit cell with lattice parameters $a =$ 2.9 nm, $b =$ 1.6 nm, $\theta \sim 75°$. The γ-network is composed of alternate rows of HBC cores and *n*-dodecyl chains. Noticeably the STM images show that three *n*-dodecyl chains are not lying on the surface and stand out-of-plane. Finally, the $\beta \rightarrow \gamma$ phase transition is accompanied by a doubling of the packing density up to 0.223 molecule/nm^2 for the γ phase.

Starting from 35 °C a fourth and final phase appears (Figure 4) to finally fully cover the surface above 45 °C. The δ-network possesses a close-packed arrangement with a hexagonal unit cell and lattice parameters $a = b =$ 1.8 nm. The Au reconstruction can still be seen as a small topographic undulation under the molecular network, Figure 4a. The STM images show that HBC cores are surrounded by bright spots, which correspond to the out-of-plane *n*-dodecyl chains (see model in Figure 4c). The HBC-C_{12} density is 0.356 molecule/nm^2. Annealing at temperatures higher than 50 °C does not lead to the formation of any novel networks.

One fundamental question is whether these phase transitions are under kinetic or thermodynamic control. The fact that the α-network is not stable at room temperature unambiguously shows that it results from a kinetic ordering of the molecules. On the contrary, once the β, γ, and δ-networks are formed at given temperatures, their respective molecular orderings do not evolve with time. This suggests that these three succes-

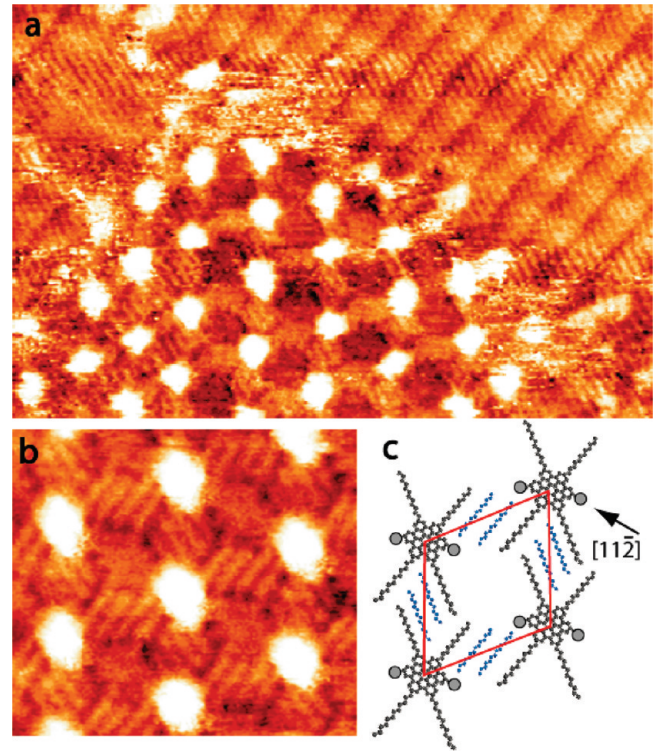

Figure 1. STM images ($V_s = -0.20$ V; $I_t = 20$ pA) of the metastable α-phase at 20 °C: (a) 30 × 20 nm^2; (b) 10 × 9 nm^2; (c) best fit molecular model of the unit cell of the α-network (0.082 molecule/nm^2). The gray circles represent out-of-plane *n*-dodecyl chains. Coadsorbed *n*-tetradecane molecules appear in blue. The arrow indicates the [$\bar{1}$12] direction of gold.

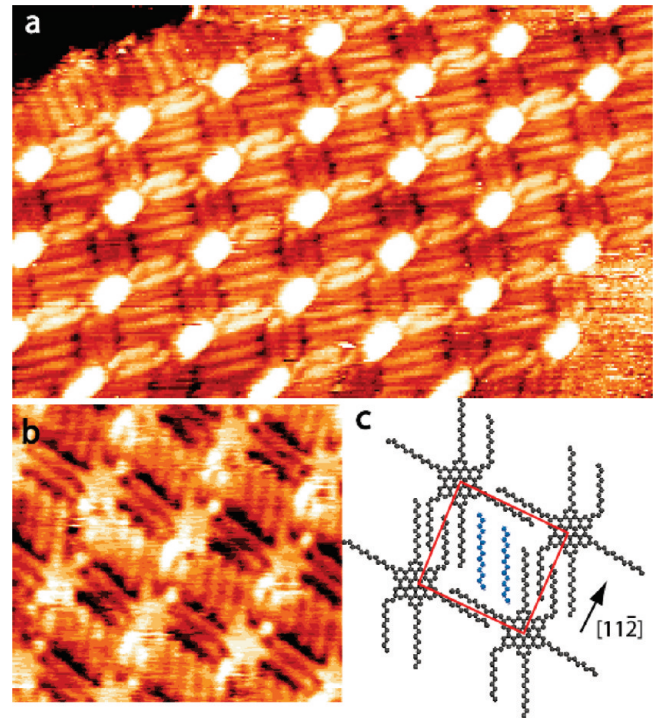

Figure 2. STM images of the β-network recorded at $T = 25$ °C: (a) 20 × 15 nm^2 ($V_s = -0.20$ V, $I_t = 50$ pA); (b) 10 × 9 nm^2 ($V_s = -0.27$ V, $I_t = 0.1$ nA); (c) unit cell of the β-network. Two coadsorbed *n*-tetradecane molecules appear in blue. Packing density = 0.111 molecule/nm^2.

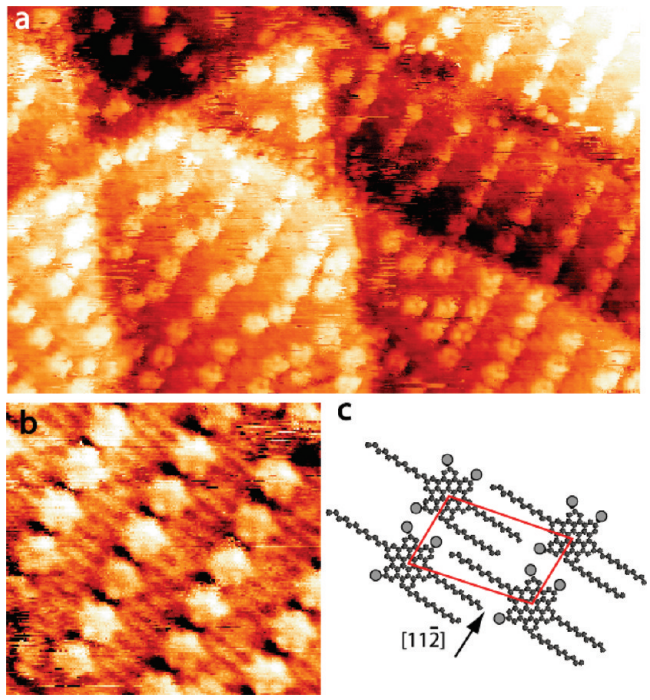

Figure 3. STM images of the γ-network recorded at 35 °C (V_s = 0.50 V, I_t = 20 pA): (a) 36 × 22 nm^2; (b) 10 × 9 nm^2; (c) unit cell of the γ-network with out-of-plane *n*-dodecyl chains represented as gray circles. Packing density = 0.223 molecule/nm^2.

sive temperature-induced structures correspond to different potential minima in the phase transition process. The δ-network is the structure obtained at the highest

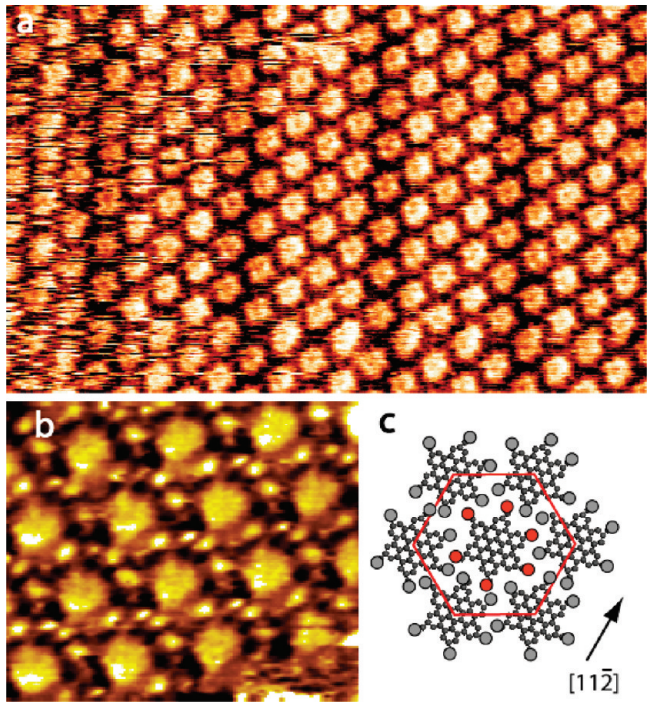

Figure 4. STM images of the δ-network recorded at 50 °C: (a) 30 × 20 nm^2, V_s = 0.60 V, I_t = 20 pA; (b) 10 × 9 nm^2, V_s = 90 mV, I_t = 20 pA; (c) unit cell of the δ-network. The six out-of-plane *n*-dodecyl chains of the central molecule are represented as red circles while they appear as gray circles for peripheral molecules. Packing density = 0.356 molecule/nm^2.

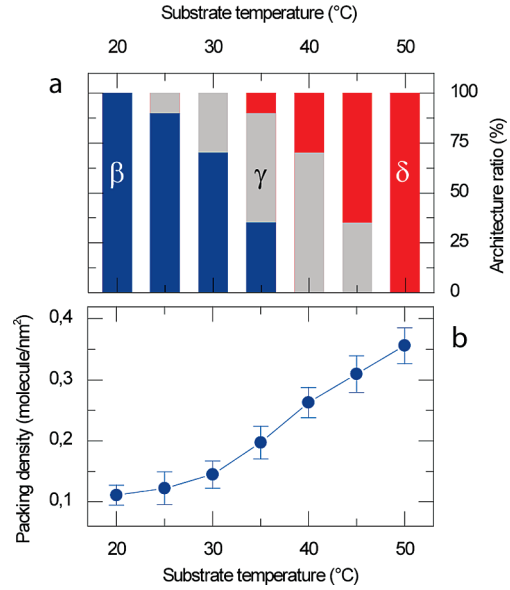

Figure 5. (a) Relative percentages of the three stable β, γ, and δ-phases of HBC-C_{12} observed on the Au(111)-(22×$\sqrt{3}$) surface at different temperatures (blue, β-phase; gray, γ-phase; red, δ-phase). (b) Plot of the HBC-C_{12} packing density at various temperatures over the 20−50 °C range.

temperatures, and once it is formed it is not possible to form any novel structure by increasing further the temperature, in contrast to what happens with the β and γ-networks. It indicates that the δ-network is thermodynamically stable, whereas the β and γ ones are metastable.

Figure 5 summarizes the above observations, with the relative percentages of the four phases observed at various temperatures and the corresponding packing densities. We did not observe any influence of the concentration of the molecule solution on the supramolecular self-assembly in contrast with other observations.[42] The number of *n*-dodecyl chains lying on the surface decreases with increasing temperatures. Six *n*-dodecyl chains are lying on the surface at 20 °C (β-network), three chains are lying on the surface at 25−45 °C (γ-network), whereas no more *n*-dodecyl chains lie on the surface above 50 °C (δ-network). The packing density was measured after 30 min of thermal annealing. Longer annealing times or decreasing the sample temperature back to 20 °C does not change the arrangement. Temperature-induced HBC-C_{12} phase transitions are therefore irreversible. This provides the possibility to finely tune the HBC-C_{12} packing density by adjusting the substrate temperature, in contrast to what happens on graphite where HBC-C_{12} phase transitions occur spontaneously with time.[32]

The STM measurements show that above room temperature adsorption of the HBC core is favored as compared with *n*-dodecyl chains. This means that the chains progressively desorb into the liquid solution with increasing temperature and are replaced by the HBC molecules. The arrangement observed at 50 °C, that is the highest temperature presented here, is the hexagonal

close-packed δ-network with no alkyl chain on the surface. This indicates that the HBC-based supramolecular structures minimize their energy by increasing HBC packing density and reducing alkyl chain adsorption. These observations suggest that energy minimization is done at the cost of molecule stress conformation permitting the alkyl chains to be out of the HBC plane. The development of theoretical models taking into account (i) the various molecule− molecule and molecule−substrate interactions, (ii) the influence of the solvent, and (iii) molecular conformational changes is necessary to evaluate the energy of the different 2D architectures that we observe experimentally here.

CONCLUSION

We show that the packing density of HBC-C_{12} 2D self-assemblies on Au(111) can be tuned by adjusting the temperature. Increasing the temperature over the 20−50 °C range induces three irreversible phase transitions ($\alpha \rightarrow \beta \rightarrow \gamma \rightarrow \delta$) and a 3-fold increase of the packing density from 0.111 to 0.356 molecule/nm^2. Importantly, cooling the samples back to room temperature after a heating experiment is not accompanied by a decrease of the packing density nor by a structural change back to the initial phase. Such temperature-controlled irreversible phase transitions are thus a versatile tool that can then be used to adjust the packing density of highly ordered functional materials in view of applications in organic electronic devices. Tuning the packing density of large disklike conjugated molecules adsorbed face-on on a surface would be an elegant way to optimize light absorption and charge transport in sandwich devices such as organic solar cells. For example, self-organization of discotic liquid crystals (LCs) such as HBC-C_{12} can be used to create, directly from solution, stable thin films for use in photovoltaic devices.[43] The columnar structure of LCs is at the origin of their 1D charge conduction and is essentially determined by the area of π-overlapping and the intercolumnar distance.[44] However the packing density of these LC columnar phases has not been optimized and results from a deposition performed at room temperature. Then, the possibility of tuning the packing density of a nanotemplate monolayer, and hence the intercolumnar distance in the LC film, by means of temperature could allow the adjustment of precisely photoexciton generation and dissociation and/or the quasi-1D transport of charge carriers along the columnar stacks.

EXPERIMENTAL SECTION

Solutions of HBC-C_{12} in *n*-tetradecane (n-$C_{14}H_{30}$, 99%, Aldrich) were prepared in a concentration range 10^{-6}−10^{-5} mol L^{-1}. A droplet of this solution was then deposited on a flame-annealed Au(111)/mica substrate. Reconstructed Au(111)-$(22\times\sqrt{3})$ surface was systematically checked using STM. STM imaging was performed at the *n*-tetradecane/Au(111) interface using a Pico-SPM scanning tunneling microscope (Molecular Imaging, Agilent Technology). The sample holder was placed inside an environmental chamber together with a small quantity of *n*-tetradecane in order to prevent evaporation. Cut Pt/Ir STM tips were used to obtain constant current images with a bias voltage applied to the sample. A homemade sample holder coupled to a Peltier element module (Supercool PE-071-20-15) was used to control the substrate temperature in the range 20−50 °C. The temperature was measured using a thermocouple connected to the sample stage (error ± 0.5 °C). STM images were recorded after heating the samples up to a selected temperature for 30 min and also after cooling down the sample to room temperature. STM images were processed and analyzed using the homemade application FabViewer.[45]

REFERENCES AND NOTES

1. Barth, J. V. Molecular Architectonic on Metal Surfaces. *Annu. Rev. Phys. Chem.* **2007**, *58*, 375–407.
2. Samori, P. Exploring Supramolecular Interactions and Architectures by Scanning Force Microscopies. *Chem. Soc. Rev.* **2005**, *34*, 551–561.
3. Elemans, J. A. A. W.; De Cat, I.; Xu, H.; De Feyter, S. Two-Dimensional Chirality at Liquid−Solid Interfaces. *Chem. Soc. Rev.* **2009**, *38*, 722–736.
4. Barth, J. V.; Costantini, G.; Kern, K. Engineering Atomic and Molecular Nanostructures at Surfaces. *Nature* **2005**, *437*, 671–679.
5. Cicoira, F.; Santato, C.; Rosei, F. Two-Dimensional Nanotemplates as Surface Cues for the Controlled Assembly of Organic Molecules. *Top. Curr. Chem.* **2008**, *285*, 203–267.
6. Piot, L.; Silly, F.; Tortech, L.; Nicolas, Y.; Blanchard, P.; Roncali, J.; Fichou, D. Long-Range Alignments of Single Fullerenes by Site-Selective Inclusion Into a Double-Cavity 2D Open Network. *J. Am. Chem. Soc.* **2009**, *131*, 12864–12865.
7. Rosei, F.; Schunack, M.; Naitoh, Y.; Jiang, P.; Gourdon, A.; Laegsgaard, E.; Stensgaard, I.; Joachim, C.; Besenbacher, F. Properties of Large Organic Molecules on Metal Surfaces. *Prog. Surf. Sci.* **2003**, *33*, 95–146.
8. Samori, P. Scanning Probe Microscopies Beyond Imaging. *J. Mater. Chem.* **2004**, *14*, 1353–1366.
9. Kudernac, T.; Lei, S. A.; Elemans, A. W.; De Feyter, S. Two-Dimensional Supramolecular Self-Assembly: Nanoporous Networks on Surfaces. *Chem. Soc. Rev.* **2009**, *38*, 402–421.
10. Elemans, J. A. A. W.; Lei, S.; De Feyter, S. Molecular and Supramolecular Networks on Surfaces: From Two-Dimensional Crystal Engineering to Reactivity. *Angew. Chem., Int. Ed.* **2009**, *48*, 7298–7333.
11. Katano, S.; Kim, Y.; Matsubara, H.; Kitagawa, T.; Kawai, M. Hierarchical Chiral Framework Based on a Rigid Adamantane Tripod on Au(111). *J. Am. Chem. Soc.* **2007**, *129*, 2511–2515.
12. Xiao, W.; Ruffieux, P.; Ait-Mansour, K.; Groning, O.; Palotas, K.; Hofer, W. A.; Groning, P.; Fasel, R. Formation of a Regular Fullerene Nanochain Lattice. *J. Phys. Chem. B* **2006**, *110*, 21394–21398.
13. Nishiyama, F.; Yokoyama, T.; Kamikado, T.; Yokoyama, S.; Mashiko, S.; Sakaguchi, K.; Kikuchi, K. Interstitial Accommodation of C_{60} in a Surface-Supported Supramolecular Network. *Adv. Mater.* **2007**, *19*, 117–120.
14. Deak, D. S.; Silly, F.; Porfyrakis, K.; Castell, M. R. Surface Ordering of Endohedral Fullerenes With $SrTiO_3$(001). *Nanotechnology* **2007**, *18*, 075301-1–075301-6.

15. Lin, X.; Nilius, N. Self-Assembly of MgPc Molecules on Polar FeO Thin Films. *J. Phys. Chem. C* **2008**, *112*, 15325. 1−9.
16. MacLeod, J. M.; Ivasenko, O.; Perepichka, D. F.; Rosei, F. Stabilization of Exotic Minority Phases in a Multicomponent Self-Assembled Molecular Network. *Nanotechnology* **2007**, *18*, 424031.
17. Zhang, H. L.; Chen, W.; Huang, H.; Chen, L.; Wee, A. T. S. Preferential Trapping of C_{60} in Nanomesh Voids. *J. Am. Chem. Soc.* **2008**, *130*, 2720.
18. Keg, P.; Lohani, A.; Fichou, D.; Lam, Y. M.; Wu, Y. L.; Ong, B. S.; Mhaisalkar, S. G. Direct Observation of Alkyl Chain Interdigitation in Conjugated Poly(Quarterthiophene) Self-Organized on Graphite Surfaces. *Macromol. Rapid Commun.* **2008**, *29*, 1197–1202.
19. Nion, A.; Jiang, P.; Popoff, A.; Fichou, D. Rectangular Nanostructuring of Au(111) Surfaces by Self-Assembly of Size-Selected Thiacrown Ether Macrocycles. *J. Am. Chem. Soc.* **2007**, *129*, 2450–2451.
20. Vidal, F.; Delvigne, E.; Stepanow, S.; Lin, N.; Barth, J. V.; Kern, K. Chiral Phase Transition in Two-Dimensional Supramolecular Assemblies of Prochiral Molecules. *J. Am. Chem. Soc.* **2005**, *127*, 10101–10106.
21. Nath, K. G.; Ivasenko, O.; Miwa, J. A.; Dang, H.; Wuest, J. D.; Nanci, A.; Perepichka, D. F.; Rosei, F. Rational Modulation of the Periodicity in Linear Hydrogen-Bonded Assemblies of Trimesic Acid on Surfaces. *J. Am. Chem. Soc.* **2006**, *128*, 4212–4213.
22. Silly, F.; Shaw, A. Q.; Briggs, G. A. D.; Castell, M. R. Epitaxial Ordering of a PTCDI−Melamine Supramolecular Network Driven by the Au(111)-(22×√3) Reconstruction. *Appl. Phys. Lett.* **2008**, *92*, 023102-1–023102-3.
23. Popoff, A.; Fichou, D. Immobilization of Paracetamol and Benzocaine Pro-drug Derivatives as Long-Range Self-Organized Monolayers on Graphite. *Colloids Surf. B:* **2008**, *63*, 153–158.
24. Xiao, W.; Feng, X.; Ruffieux, P.; Gröning, O.; Müllen, K.; Fasel, R. Self-Assembly of Chiral Molecular Honeycomb Networks on Au(111). *J. Am. Chem. Soc.* **2008**, *130*, 8910–8912.
25. Lackinger, M.; Heckl, W. M. Carboxylic Acids: Versatile Building Blocks and Mediators for Two-Dimensional Supramolecular Self-Assembly. *Langmuir* **2009**, *25*, 11307–11321.
26. Silly, F.; Shaw, A. Q.; Castell, M. R.; Briggs, G. A. D.; Mura, M.; Martsinovich, N.; Kantorovich, L. Melamine Structures on the Au(111) Surface. *J. Phys. Chem. C* **2008**, *112*, 11476–11480.
27. Piot, L.; Marie, C.; Feng, X.; Müllen, K.; Fichou, D. Hierarchical Self-Assembly of Edge-On Nanocolumnar Superstructures of Large Disc-like Molecules. *Adv. Mater.* **2008**, *20*, 3854–3858.
28. Piot, L.; Marie, C.; Dou, X.; Feng, X.; Müllen, K.; Fichou, D. Growth of Long, Highly Stable, and Densely Packed Worm-like Nanocolumns of Hexa-*peri*-hexabenzocoronenes *via* Chemisorption on Au(111). *J. Am. Chem. Soc.* **2009**, *131*, 1378.
29. Xu, L. P.; Yan, C. J.; Wan, L. J.; Jiang, S. G.; Liu, M. H. Light-Induced Structural Transformation in Self-Assembled Monolayer of 4-(Amyloxy)cinnamic Acid Investigated with Scanning Tunneling Microscopy. *J. Phys. Chem. B* **2005**, *109*, 14773–14778.
30. Mougous, J. D.; Brackley, A. J.; Foland, K.; Backer, R. T.; Patrick, D. L. Formation of Uniaxial Molecular Films by Liquid-Crystal Imprinting in a Magnetic Field. *Phys. Rev. Lett.* **2000**, *84*, 2742–2745.
31. Wan, L. J.; Noda, H.; Wang, C.; Bai, C. L.; Osawa, M. Controlled Orientation of Individual Molecules by Electrode Potentials. *ChemPhysChem.* **2001**, *2*, 617–619.
32. Piot, L.; Marchenko, A.; Wu, J.; Müllen, K.; Fichou, D. Structural Evolution of Hexa-*peri*-hexabenzocoronene Adlayers in Heteroepitaxy on *n*-Pentacontane Template Monolayers. *J. Am. Chem. Soc.* **2005**, *127*, 16245–16250.
33. Hong, X.; Minoia, A.; Tomovic, Z.; Lazzaroni, R; Meijer, E. W.; Schenning, A. P. H. J.; De Feyter, S. A Multivalent Hexapod: Conformational Dynamics of Six-Legged Molecules in Self-Assembled Monolayers at a Solid-Liquid Interface. *ACS Nano* **2009**, *3*, 1016–1024.
34. Lackinger, M.; Heckl, W. M. Carboxylic Acids: Versatile Building Blocks and Mediators for Two-Dimensional Supramolecular Self-Assembly. *Langmuir* **2009**, *25*, 11307–11321.
35. Lei, S.; Tahara, K.; De Schryver, F. C.; Van der Auweraer, M.; Tobe, Y.; De Feyter, S. One Building Block, Two Different Supramolecular Surface-Confined Patterns: Concentration in Control at the Solid−Liquid Interface. *Angew. Chem., Int. Ed.* **2008**, *47*, 2964–2968.
36. Huang, Y. L.; Chen, W.; Li, H.; Ma, J.; Pflaum, J.; Wee, A. T. S. Tunable Two-Dimensional Binary Molecular Networks. *Small* **2010**, *6*, 70–75.
37. Li, C. J.; Zeng, Q. D.; Liu, Y. H.; Wan, L. J.; Wang, C.; Wang, C. R.; Bai, C. L. Evidence of a Thermal Annealing Effect on Organic Molecular Assembly. *ChemPhysChem* **2003**, *4*, 857–859.
38. Silly, F.; Shaw, A. Q.; Porfyrakys, K.; Briggs, G. A. D.; Castell, M. R. Pairs and Heptamers of C_{70} Molecules Ordered *via* PTCDI-Melamine Supramolecular Networks. *Appl. Phys. Lett.* **2007**, *91*, 253109-1–253109-3.
39. Klappenberger, F.; Weber-Bargioni, A.; Auwärter, W.; Marschall, M.; Schiffrin, A.; Barth, J. V. Temperature Dependence of Conformation, Chemical State, and Metal-Directed Assembly of Tetrapyridyl-Porphyrin on Cu(111). *J. Chem. Phys.* **2008**, *129*, 214702-1–214702-3.
40. Orzali, T.; Forrer, D.; Sambi, M.; Vittadini, A.; Casarin, M.; Tondello, E. Temperature-Dependent Self-Assemblies of C_{60} on (1×2)-Pt(110): A STM/DFT Investigation. *J. Phys. Chem. C* **2008**, *112*, 378–390.
41. Treossi, E.; Liscio, A.; Feng, X.; Palermo, V.; Müllen, K.; Samori, P. Temperature-Enhanced Solvent Vapor Annealing of a C_3 Symmetric Hexa-*peri*-hexabenzocoronene: Controlling the Self-Assembly from Nano- to Macroscale. *Small* **2009**, *5*, 112–119.
42. Mamdouh, W.; Uji-i, H.; Ladislaw, J. S.; Dulcey, A. E.; Percec, V.; De Schryver, F. C.; De Feyter, S. Solvent Controlled Self-Assembly at the Liquid−Solid Interface Revealed by STM. *J. Am. Chem. Soc.* **2006**, *128*, 317–325.
43. Schmidt-Mende, L.; Fechtenkötter, A.; Müllen, K.; Moons, E.; Friend, R. H.; MacKenzie, J. D. Self-Organized Discotic Liquid Crystals for High-Efficiency Organic Photovoltaics. *Science* **2001**, *293*, 1119–1122.
44. Sergeyev, S.; Pisula, W.; Geerts, Y. H. Discotic Liquid Crystals: A New Generation of Organic Semiconductors. *Chem. Soc. Rev.* **2007**, *36*, 1902–1929.
45. Silly, F. A Robust Method for Processing Scanning Probe Microscopy Images and Determining Nano-object Position and Dimensions. *J. Microsc. (Oxford)* **2009**, *236*, 211–218.